

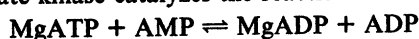
Solution Structure of the 45-Residue MgATP-Binding Peptide of Adenylate Kinase As Examined by 2-D NMR, FTIR, and CD Spectroscopy[†]

David C. Fry,^{‡§} D. Michael Byler,^{||} Heino Susi,^{||} Eleanor M. Brown,^{||} Stephen A. Kuby,[⊥] and Albert S. Mildvan^{*,‡}
 Department of Biological Chemistry, The Johns Hopkins University School of Medicine, 725 North Wolfe Street, Baltimore, Maryland 21205, Eastern Regional Research Center of the U.S. Department of Agriculture, Philadelphia, Pennsylvania 19118, and Laboratory for the Study of Hereditary and Metabolic Diseases and Departments of Biological Chemistry and Medicine, University of Utah, Salt Lake City, Utah 84108

Received August 31, 1987; Revised Manuscript Received December 15, 1987

ABSTRACT: The structure of a synthetic peptide corresponding to residues 1–45 of rabbit muscle adenylate kinase has been studied in aqueous solution by two-dimensional NMR, FTIR, and CD spectroscopy. This peptide, which binds MgATP and is believed to represent most of the MgATP-binding site of the enzyme [Fry, D. C., Kuby, S. A., & Mildvan, A.S. (1985) *Biochemistry* 24, 4680–4694], appears to maintain a conformation similar to that of residues 1–45 in the X-ray structure of intact porcine adenylate kinase [Sachsenheimer, W., & Schulz, G. E. (1977) *J. Mol. Biol.* 114, 23–26], with 42% of the residues of the peptide showing NOEs indicative of ϕ and ψ angles corresponding to those found in the protein. The NMR studies suggest that the peptide is composed of two helical regions of residues 4–7 and 23–29, and three stretches of β -strand at residues 8–15, 30–32, and 35–40, yielding an overall secondary structure consisting of 24% α -helix, 38% β -structure, and 38% aperiodic. Although the resolution-enhanced amide I band of the peptide FTIR spectrum is broad and rather featureless, possibly due to disorder, it can be fit by using methods developed on well-characterized globular proteins. On this basis, the peptide consists of $35 \pm 10\%$ β -structure, $60 \pm 12\%$ turns and aperiodic structure, and not more than 10% α -helix. The CD spectrum is best fit by assuming the presence of at most 13% α -helix in the peptide, $24 \pm 2\%$ β -structure, and $66 \pm 4\%$ aperiodic. The inability of the high-frequency FTIR and CD methods to detect helices in the amount found by NMR may result from the short helical lengths as well as from static and dynamic disorder in the peptide. Upon binding of MgATP, numerous conformational changes in the backbone of the peptide are detected by NMR, with smaller alterations in the overall secondary structure as assessed by CD. Detailed assignments of resonances in the peptide spectrum and intermolecular NOEs between protons of bound MgATP and those of the peptide, as well as chemical shifts of peptide resonances induced by the binding of MgATP, are consistent with the previously proposed binding site for MgATP on adenylate kinase.

Adenylate kinase catalyzes the reaction



The enzyme contains two distinct nucleotide binding sites: the MgATP site, which binds MgATP and MgADP, and the AMP site, which is specific for AMP and uncomplexed ADP.

We have recently examined the MgATP site in a series of NMR¹ studies on rabbit muscle adenylate kinase (Fry et al., 1985) and on a synthetic peptide, corresponding to residues 1–45 of the enzyme, that binds metal-ATP with comparable

[†]This work was supported by National Institutes of Health Grants DK28616 (to A.S.M.) and DK07824 (to S.A.K.).

[‡]The Johns Hopkins University School of Medicine.

[§]Present address: Department of Physical Chemistry, Hoffmann-La Roche, Inc., Nutley, NJ 07110.

^{||}Eastern Regional Research Center of the U.S. Department of Agriculture.

[⊥]University of Utah.

¹ Abbreviations: NMR, nuclear magnetic resonance; NOE, nuclear Overhauser effect; T_1 , longitudinal relaxation time; Cr^{3+} ATP, β , γ -bisubstituted chromium adenosine triphosphate; FTIR, Fourier transform infrared; CD, circular dichroism; COSY, two-dimensional J -correlated NMR spectroscopy; NOESY, two-dimensional NOE NMR spectroscopy; RMS, root mean square; 2-D, two dimensional; DSS, sodium 4,4-dimethyl-4-silapentanesulfonate; A/D, analogue to digital; $d_{\alpha\text{N}}$, d_{NN} , and $d_{\beta\text{N}}$ (Wüthrich et al., 1984), short, NOE-producing distances between the NH proton of a given residue and, respectively, the C α H, NH, or C β H proton of its N-terminal neighbor.

affinity (Hamada et al., 1979). The conformation of bound MgATP was determined through the use of time-dependent intramolecular NOEs and was found to be nearly identical on both the peptide and the intact enzyme. The location of bound metal-ATP on adenylate kinase was assessed by using intermolecular distances obtained by two methods—the paramagnetic probe- T_1 technique utilizing Cr^{3+} ATP and a systematic acquisition of intermolecular NOEs using MgATP. These experiments were performed on both the enzyme and the peptide. This distance information was used to position metal-ATP into the X-ray structure of porcine adenylate kinase (Sachsenheimer & Schulz, 1977) by use of a computer graphics system. Distances obtained on the peptide were incorporated by assuming that the solution structure of the peptide was comparable to that of residues 1–45 in the X-ray structure of the intact enzyme. This assumption yielded a single metal-ATP site that accommodated all of the NMR data and that agreed well with substrate specificity and sequence homology observations on adenylate kinase (Fry et al., 1986a).

The recent development of a variety of two-dimensional NMR methods has made possible the direct determination of solution structures of peptides consisting of up to approximately 100 residues (Williamson et al., 1985; Wand & Englander, 1986; Holak & Prestegard, 1986; van de Ven & Hilbers, 1986a). Therefore, we have been able to examine in detail the solution structure of the 45-residue peptide by applying such techniques. The structure of the peptide was evaluated both with and without bound MgATP. We show that the secondary structure of the free peptide 1–45 in solution as determined by NMR approximates that of residues 1–45 in crystals of intact adenylate kinase and that significant structural changes in the peptide are detected upon binding of MgATP. We have also utilized CD and FTIR spectroscopy as independent probes of the conformation. A preliminary report of this work has been published (Fry et al., 1986b).

EXPERIMENTAL PROCEDURES

Material. The synthetic peptide corresponding to residues 1–45 of rabbit muscle adenylate kinase was prepared and purified as previously described (Fry et al., 1985).

NMR Spectroscopy. All NMR experiments were performed by observing protons at 10 °C using 16-bit A/D conversion and quadrature phase detection. Preliminary one- and two-dimensional experiments were performed at 250 MHz on a Bruker WM-250. Final sets of two-dimensional experiments were performed on a Bruker WM-500 spectrometer at the New England NMR Facility at Yale University. Initial processing of data acquired at Yale utilized the FTNMR software package written by Dr. Dennis Hare.

NMR samples contained 4–5 mM peptide, 150 mM NaCl, and 40 mM β -mercaptoethanol in 90% H_2O /10% D_2O at pH 5.6 in a volume of 400 μL . Samples utilized to study MgATP binding also contained MgATP at a 1:1 concentration ratio with peptide.

The two-dimensional NMR experiments used to completely assign the resonances of the peptide and obtain structural information were COSY (Aue et al., 1976; Bax & Freeman, 1981) and NOESY (Jeener et al., 1979; Anil Kumar et al., 1980), taken at 500 MHz. These experiments were performed by using 90° pulses and sweep widths of 4386 Hz in both dimensions, collected as 512 FIDs each with 2K data points (COSY) or 256 FIDs each with 1K data points (NOESY), with 128 (COSY) or 208 (NOESY) transients plus two dummy transients per FID, in an acquisition time of 0.23 (COSY) or 0.12 (NOESY) s/transient. An additional re-

laxation delay of 0.9 s preceded each transient. Suppression of the H_2O resonance was achieved by direct irradiation at 10 dB below 0.2 W during the relaxation delay and at 50 dB below 0.2 W during the mixing time in NOESY experiments. The mixing time in the NOESY experiments during which NOEs were allowed to develop was 0.4 s and was varied randomly by $\pm 5\%$ to avoid COSY-type cross-peaks (Macura et al., 1981). Two-dimensional NMR data were zero-filled to a final size of 2K \times 2K points (COSY) or 1K \times 1K points (NOESY) and Fourier transformed, using multiplication by unshifted sine-bell functions in both dimensions.

Preliminary experiments at 250 MHz, such as determining the T_1 values of the peptide resonances and the exchange rates of the NH protons with H_2O , were performed in order to determine suitable recycle times at 500 MHz and a temperature at which NH resonance intensities would not be significantly reduced by presaturation of the H_2O resonance. In addition, a series of NOESY experiments were performed with various mixing times, ranging from 50 to 700 ms, until a value was established (400 ms) at which cross-peak intensities were reasonably high and secondary NOEs were not yet manifested.

FTIR Spectroscopy. Samples for FTIR contained 8.4 mM peptide, 150 mM NaCl, 40 mM β -mercaptoethanol at pH 5.6 in a volume of 50 μL , and MgATP, when present, at a concentration equivalent to that of the peptide. Samples were placed into D_2O by lyophilization twice. Spectra of each solution were obtained at 29.5 ± 1 °C using a variable path length infrared cell equipped with CaF_2 windows; the path length was set to 0.075 mm. The interferometer is a Nicolet 7199 equipped with a water-cooled Globar source and a wide-range mercury/cadmium/telluride detector. To obtain spectra with a sufficient signal-to-noise ratio for resolution enhancement, 4000 interferograms for each sample were co-added, phase corrected, zero-filled one time, apodized with the Happ-Genzel function, and Fourier transformed. The data were collected at a nominal instrument resolution of 2 cm^{-1} (Byler & Susi, 1986).

CD Spectroscopy. CD spectra at room temperature (25 ± 1 °C) were acquired by using a Jasco 41C spectropolarimeter equipped with a data processor and calibrated with *d*-10-camphorsulfonic acid according to the procedure of Chen and Yang (1977). A 0.5 mg/mL peptide solution containing 0.15 M NaCl at pH 5.6 was placed in a 0.02-cm path length cylindrical cell. The molar peptide concentration was estimated from the [^{14}C] on the basis of the presence of [^{14}C]glycine at position 33 (Fry et al., 1985). The average of 16 scans over the 260–185-nm range at a sensitivity of 5×10^{-3} deg/cm was obtained by using a time constant of 1 s, a 0.2-nm spectral step, and a 2-nm bandwidth. MgATP (320 μM) was used to observe the effect of ATP on the peptide conformation. CD spectra at 2.0 ± 0.1 °C and at 10.0 ± 0.1 °C were acquired by use of an Aviv Model 60DS spectropolarimeter equipped with a Neslab Endocal temperature-regulated circulating bath. The spectra were obtained over the same spectral range with a dwell time of 0.5 s, a 0.5-nm spectral step size, and a 1.5-nm bandwidth at a peptide concentration of 0.9 mg/mL in a 0.01-cm path length cell. An equivalent concentration of MgATP (200 μM) was added under conditions otherwise as described above. Spectra were manually or instrumentally digitized and smoothed once and are presented in terms of the mean residue ellipticity $[\theta]_{\text{MRW}}$. Estimates of secondary structure were obtained by comparing experimental spectra with published CD basis sets (Chen et al., 1974; Bolotina et al., 1980; Stone et al., 1985) using a multiple linear regression computer program.

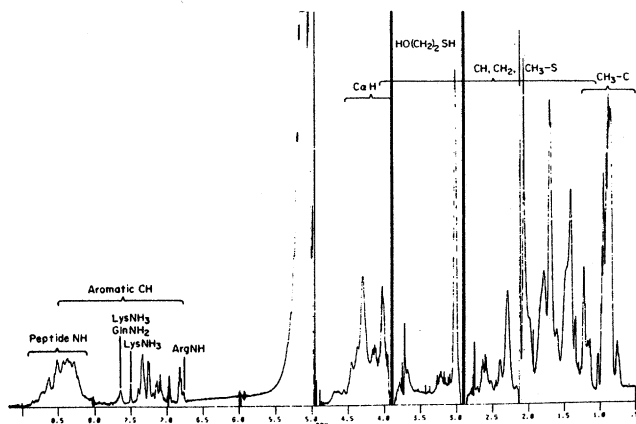


FIGURE 1: Proton spectrum at 500 MHz of rabbit muscle adenylate kinase synthetic peptide 1-45. The sample contained 4.0 mM peptide, 150 mM NaCl, 40 mM β -mercaptoethanol, 10% D_2O , and 90% H_2O at pH 5.6 and 10 °C. The spectrum was obtained by using 90° pulses and a sweep width of 5000 Hz, with preirradiation of the water resonance at 10 dB below 0.2 W for 3.0 s, collected as 256 transients of 16K data points each. The spectrum is resolution enhanced.

RESULTS AND DISCUSSION

Assignment of NMR Resonances. The 500-MHz 1H NMR spectrum of peptide 1-45 in 90% $H_2O/10\%$ D_2O is shown in Figure 1. Assignment of individual resonances (Table I) was accomplished primarily from 1H COSY and NOESY spectra by using the strategy developed by K. Wüthrich and co-workers (Wagner & Wüthrich, 1982; Wüthrich et al., 1984) and applied successfully in several studies of peptides and small proteins (Weber et al., 1985a; Wand & Englander, 1986; Wagner et al., 1986; van de Ven & Hilbers, 1986b). The resonances were initially identified in terms of residue type on the basis of COSY connectivity patterns.

Figure 2 shows the COSY spectrum in the region of the aliphatic protons and demonstrates for two types of amino acid residue how it is possible, guided by general chemical shift information derived from model peptides (Bundi & Wüthrich, 1979; Wüthrich, 1986), to trace a characteristic connectivity pattern for each residue in the peptide. COSY connectivities were also used to assign resonances in the aromatic region of the spectrum, as shown in Figure 3. The assignment process in peptide 1-45 was aided by information obtained in earlier one-dimensional experiments, particularly a full pH titration study (Fry et al., 1985), as well as by comparison to a smaller piece of the peptide, comprised of residues 31-45, which had previously been completely assigned by one- and two-dimensional methods (Fry et al., 1985). Such information also allowed assignment of resonances that gave no COSY cross-peaks, such as histidine ring protons and the S- CH_3 protons of methionine.

The aromatic residues were assigned by matching ring protons, specifically identified on the basis of chemical shift, to aliphatic protons through use of the NOESY spectrum. In each aromatic residue, an NOE was observed between a $C\beta H$ proton and the nearest ring protons of the same residue (C2, C6H in Phe and Tyr; C4H in His), thus allowing complete assignments to be made. Several other residues were readily identified by type on the basis of chemical shift and obvious COSY linkages (Gly, Ser, Asp, Cys, Pro) and with the help of pH titration (Asp, Glu, His, Tyr, Lys) and comparison to peptide 31-45 (Glu, Ala). Valine residues were unambiguously assigned through the observation of NOEs from methyl protons to NH protons and the tracing of COSY connectivities ($C\gamma H_3$ - $C\beta H$ - CaH -NH) between these resonances. Isoleucine residues were assigned by the observation of NOEs

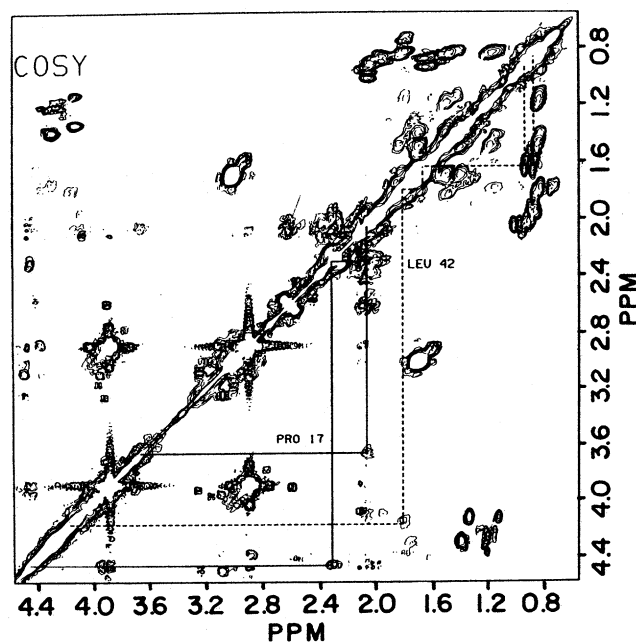


FIGURE 2: Aliphatic region of the COSY spectrum of peptide 1-45. Representative J -connectivity patterns for two residues are shown: proline 17 (CaH - $C\beta H_2$ - $C\gamma H_2$ - $C\delta H_2$) and leucine 42 [CaH - $C\beta H_2$ - $C\gamma H$ - $(C\delta H_3)_2$]. The spectrum was obtained by using the pulse sequence of Bax and Freeman (1981), 90° pulses, and a sweep width of 4386 Hz in both dimensions, collected as 512 FIDs of 2K data points each with 128 scans plus 2 dummy scans per FID. The water resonance was suppressed by preirradiation for 0.9 s at 10 dB below 0.2 W. The data were zero filled to a final size of $2K \times 2K$ points and transformed, using multiplication by sine-bell functions in both dimensions.

from $C\gamma H_3$ resonances to NH resonances² and the tracing of $C\gamma H_3$ - $C\beta H$ - CaH -NH COSY connectivities. The $C\gamma H_2$ and $C\delta H_3$ resonances were subsequently assigned in COSY spectra by tracing from $C\beta H$ to the upfield member of the $C\gamma H_2$ pair and then to $C\delta H_3$. The downfield $C\gamma H$ resonance was identified by its COSY cross-peaks to both $C\delta H_3$ and the upfield $C\gamma H$. Cross-peaks between $C\beta H$ and the downfield $C\gamma H$ were not observed for any isoleucine residue. Leucine residues were assigned in COSY spectra by tracing connectivities from the methyl resonances that were not assigned to valines or isoleucines.

Problems of overlap among the remaining β resonances (Glu, Met, Leu, Lys, Arg) and threonine γ resonances were resolved during the process of forming a self-consistent set of sequential assignments from NOESY data (described later). NOEs between NH and $C\beta H$ protons that were also linked through COSY connectivity (NH- CaH - $C\beta H$) were used to verify several of these assignments.² Resonances that could not be completely and specifically assigned were those of methylene CH_2 and side-chain NH protons of lysine and arginine. Following the nearly complete identification of CaH resonances of the peptide, the amide NH of each resonance

² A subsequent phase-sensitive relay-COSY experiment of the type described by Weber et al. (1985b) at 400 MHz, using a Varian XL400 spectrometer, a 36-ms mixing time, and otherwise identical conditions, confirmed the validity of this strategy for making assignments by residue type. However, the specific sequential assignments, made amidst the extreme overlap exhibited by the peptide resonances, could not be confirmed by additional experiments, since more NOEs of a long-range nature [e.g., $i - (i + 3)$ backbone NOEs] would be the only information capable of resolving such a problem, and these NOEs do not exist. Therefore, in the cases of multiple like residues, while confidence in the assignments by residue type is high, the sequential assignments, though fully consistent with the data, cannot be rigorously proven as definitive.

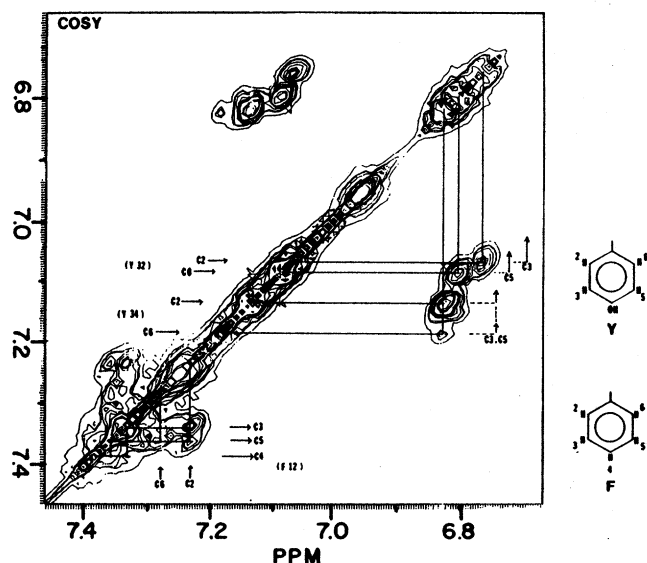


FIGURE 3: Aromatic region of the COSY spectrum of peptide 1-45. The J -connectivities of the ring protons are shown for tyrosines 32 and 34 and phenylalanine 12.

was assigned by coupling connectivity to its intraresidual CaH . This region of the COSY spectrum, the so-called "fingerprint", is shown in Figure 4.

Advancement of assignments from residue type to specific residue number relied upon knowledge of the sequence of the synthesized peptide and on the method of sequential identification proposed by Wüthrich et al. (1984). According to this method, which was developed from statistical studies of protein X-ray structures, for all sterically allowed combinations of the ϕ and ψ dihedral angles along the peptide chain, every NH proton should be $\leq 3 \text{ \AA}$ from either the CaH (d_{CaN}) or NH

(d_{NN}) of its N-terminal neighbor. Ideally, then, one should expect each NH resonance to produce an NOE to either the CaH or NH resonance of its N-terminal neighbor. In practice, this pattern has usually, though not unfailingly, been observed in the NOESY spectra of the large peptides and proteins studied by 2-D NMR (Weber et al., 1985a; Wagner et al., 1986; van de Ven & Hilbers, 1986b). It has also been noted that, depending upon the structure present, NH resonances can have numerous intraresidual and interresidual NOEs outside of this sequential pattern and that anticipated NH-to- CaH or NH-to-NH NOEs may both be present or may both be absent. Therefore, in the present case, sequential assignments were made by evaluating observed NOESY cross-peaks in the following systematic manner. First, the region of NH-to- CaH NOEs was considered, as shown in Figure 5. NOEs were sought from any of the assigned NH resonances to resonances in the CaH region, and assignments of NH and CaH resonances were used in attempts to explain these NOEs in terms of neighboring residues. All but two of the neighboring pairs of residues in peptide 1-45 are unique in the sequence, so problems of multiple possible explanations for NOEs due to chemical shift overlap were usually resolved by such neighbor identification. Of the residues whose aliphatic protons were clearly assigned in this manner (Phe, His, Tyr, Gly, Val, Ile, Asp, Cys, Ser), several are positioned next to one another in the sequence and served as linked reference points in attempting to trace sequential NOESY connectivities. For example, sets of NOEs were found to describe the stretches 10-12 (Ile-Ile-Phe), 13-15 (Val-Val-Gly), and 29-34 (Val-His-Lys-Tyr-Gly-Tyr). Other stretches were assigned by attempting to maximize the extent of NOE linkage and keep the overall assignment set self-consistent. NOEs in the NOESY fingerprint (Figure 5) that were not of the sequential CaH -NH type were cataloged as "nonsequential" effects

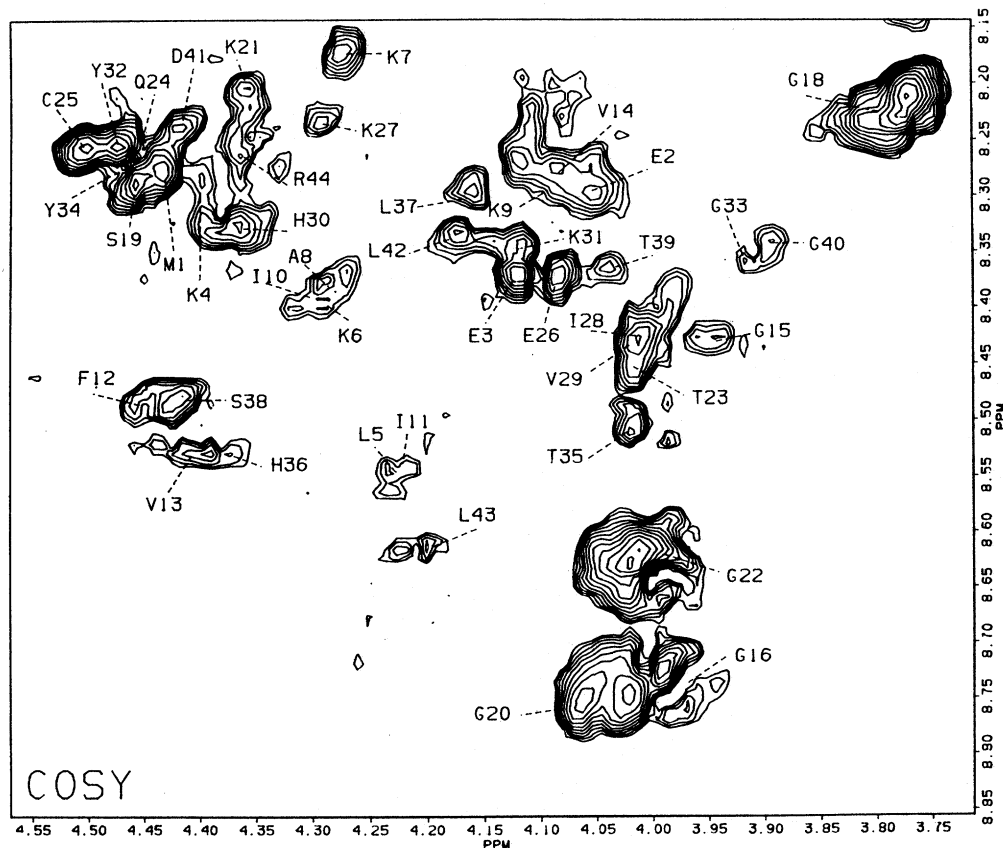


FIGURE 4: Region of NH- CaH connectivities in the COSY spectrum of peptide 1-45. The NH- CaH cross-peak for each residue is identified by the one-letter amino acid code and its position number in the peptide sequence. M1 is actually *N*-acetyl-Met.

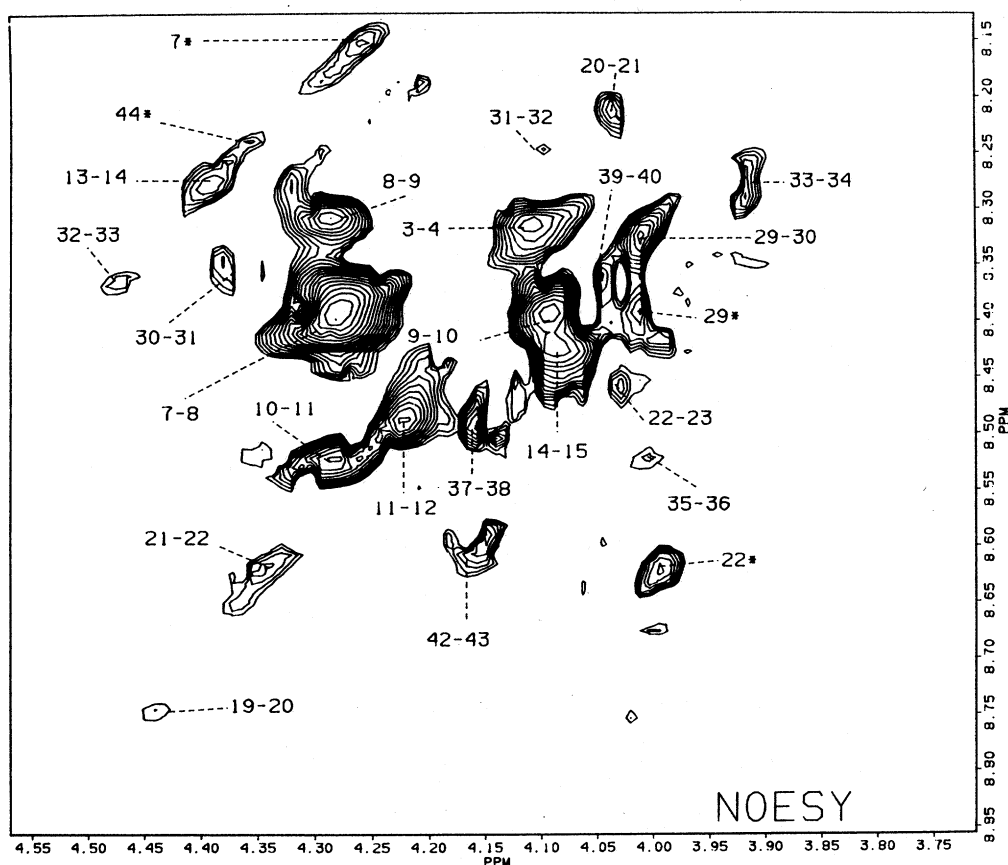


FIGURE 5: Region of NH-C α H NOEs in the NOESY spectrum of peptide 1-45. Sequential $d_{\alpha N}$ NOEs between the C α H of residue i and the NH of residue $i + 1$ are designated $i - (i + 1)$. NOEs identified by a single number and asterisk represent intraresidual effects, which are listed in Table II. The spectrum was obtained by using the pulse sequence of Anil Kumar et al. (1980), 90° pulses, and a sweep width of 4386 Hz in both dimensions, collected as 256 FIDs of 1K data points each with 208 scans plus 2 dummy scans per FID. The water resonance was suppressed by direct preirradiation for 0.9 s at 10 dB below 0.2 W and irradiation at 50 dB below 0.2 W during the mixing time. The mixing time for generation of NOEs was 0.4 s, which was varied randomly within $\pm 5\%$. The data set was zero-filled to a final size of 1K \times 1K points and transformed, using sine-bell multiplication in both dimensions.

(discussed later). An ultimate assignment scheme was sought that produced a minimal number of such nonsequential effects. It was then assumed that NH resonances which did not display an NOE to any C α H should produce an NOE to the NH resonance of a neighboring residue. Therefore, such effects were sought in the NH-NH region of the NOESY spectrum, which is shown in Figure 6. Clearly observable NOEs of this type were found for six residue pairs. The possible remaining NOEs in this region were not considered because noise ridges and the wide spread of the diagonal partially obscured these cross-peaks or hindered their verification as true NOEs. A third type of sequential NOE which has often been utilized (Weber et al., 1985a; Williamson et al., 1984; Holak & Prestegard, 1986), namely that between the NH and one C β H proton of its N-terminal neighbor ($d_{\beta N}$), was also sought for each residue pair (Figure 7).

By use of this strategy, nearly every proton in the NMR spectrum of peptide 1-45 was specifically assigned by residue number as listed in Table I.² The types of NOE connectivities observed between pairs of residues, upon which the sequential assignments were based, are outlined in Figure 8. Residues exhibiting no such sequential connectivities were assigned by default. We attribute the ability to assign the peptide with reasonable certainty, despite the small range of chemical shifts exhibited by each type of proton, to the fortuitously even distribution of residue types in the peptide sequence, with the exception of the seven lysines. The C γ H₂, C δ H₂, C ϵ H₂, and NH₃⁺ resonances of the individual lysines could not be clearly assigned because of spectral overlap.

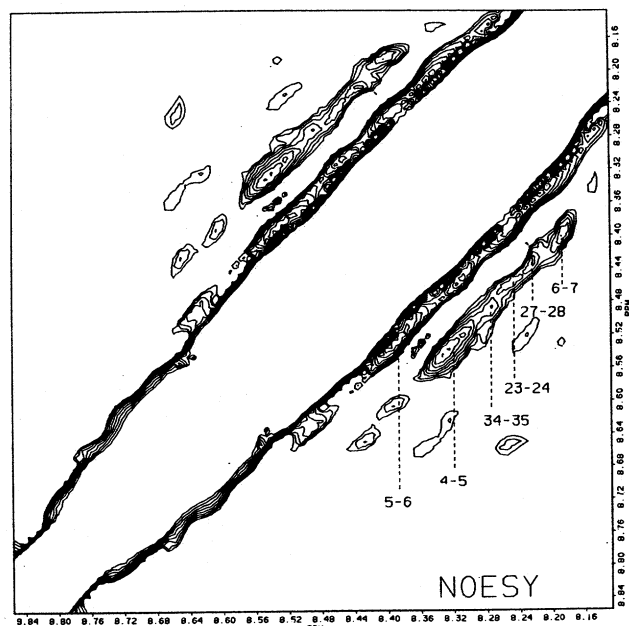


FIGURE 6: Region of NH-NH NOEs in the NOESY spectrum of peptide 1-45. Sequential d_{NN} NOEs between the NH of residue i and the NH of residue $i + 1$ are designated $i - (i + 1)$.

Structural Information from NMR Spectroscopy: Secondary Structure. Our previous assumption that peptide 1-45 maintained a regular, defined globular structure in solution was based on a number of observations (Fry et al., 1985). The

SOLUTION STRUCTURE OF MGATP-BINDING PEPTIDE

 Table I: Chemical Shifts of Proton Resonances in the NMR Spectrum of Peptide 1-45^a

residue	NH	CaH	CβH	CγH _n	CδH _n	CεH _n	other
1 N-Ac-Met	8.28	4.43	2.00	2.61			S-CH ₃ , 2.12; N-Ac, 2.12
2 Glu	8.29	4.05	2.08	2.45			
3 Glu	8.37	4.12	2.06	2.45			
4 Lys	8.29	4.40	1.60	<i>b</i>	<i>c</i>	<i>d</i>	NH ₃ , <i>e</i>
5 Leu	8.54	4.24	1.84, 1.70	2.03	0.92		
6 Lys	8.39	4.29	1.70	<i>b</i>	<i>c</i>	<i>d</i>	NH ₃ , <i>e</i>
7 Lys	8.17	4.28	1.73	<i>b</i>	<i>c</i>	<i>d</i>	NH ₃ , <i>e</i>
8 Ala	8.38	4.30	1.39				
9 Lys	8.30	4.11	1.78	<i>b</i>	<i>c</i>	<i>d</i>	NH ₃ , <i>e</i>
10 Ile	8.42	4.29	1.84	CH ₂ , 1.50, 1.21; CH ₃ , 0.89	0.87		
11 Ile	8.53	4.23	1.79	CH ₂ , 1.38, 1.16; CH ₃ , 0.84	0.84		
12 Phe	8.49	4.45	3.06, 2.95				ring C2H, 7.24; ring C3H, 7.34; ring C4H, 7.39; ring C5H, 7.36; ring C6H, 7.28
13 Val	8.53	4.39	2.07	0.95			
14 Val	8.28	4.08	1.95	0.90, 0.87			
15 Gly	8.43	3.95, 3.10					
16 Gly	8.75	3.96, 3.17					
17 Pro		4.45	2.32, 2.24	2.08		3.66	
18 Gly	8.21	3.77, 2.78					
19 Ser	8.29	4.46	3.95, 3.88				
20 Gly	8.74	4.07, 4.02					
21 Lys	8.20	4.36	1.86	<i>b</i>	<i>c</i>	<i>d</i>	NH ₃ , <i>e</i>
22 Gly	8.62	4.02, 3.98					
23 Thr	8.45	4.02	4.25	1.20			
24 Gln	8.26	4.46	2.09, 2.00	2.31			NH ₂ , 7.65, 6.96
25 Cys	8.25	4.50	3.24, 3.08				
26 Glu	8.34	4.08	2.12	2.39			
27 Lys	8.23	4.30	1.75	<i>b</i>	<i>c</i>	<i>d</i>	NH ₃ , <i>e</i>
28 Ile	8.44	4.02	1.80	CH ₂ , 1.43, 1.18; CH ₃ , 0.87	0.78		
29 Val	8.43	4.02	2.09	1.02, 0.98			
30 His	8.33	4.37	2.89				ring C2H, 8.51; ring C4H, 6.92
31 Lys	8.34	4.12	1.82	<i>b</i>	<i>c</i>	<i>d</i>	NH ₃ , <i>e</i>
32 Tyr	8.25	4.47	3.03, 2.90				ring C2H, 7.06; ring C3H, 6.76; ring C5H, 6.80; ring C6H, 7.08
33 Gly	8.36	3.92, 3.25					
34 Tyr	8.27	4.47	3.00, 2.88				ring C2H, 7.13; ring C3H, 6.82; ring C5H, 6.82; ring C6H, 7.18
35 Thr	8.50	4.02	4.36	1.23			
36 His	8.53	4.37	3.09, 2.89				ring C2H, 8.63; ring C4H, 7.02
37 Leu	8.29	4.16	1.79, 1.14	1.58	0.92		
38 Ser	8.48	4.42	3.95, 3.89				
39 Thr	8.36	4.04	4.32	1.13			
40 Gly	8.34	3.90, 2.59					
41 Asp	8.24	4.42	2.59, 2.53				
42 Leu	8.33	4.17	1.80, 1.33	1.65	0.96, 0.90		
43 Leu	8.61	4.20	1.78, 1.21	1.49	0.84		
44 Arg	8.26	4.37	1.77	1.60	2.90		NεH, 6.83; NH, <i>f</i>
45 Ala	8.04	4.12	1.34				

^aChemical shifts are reported in ppm from external DSS. The sample was maintained at 10 °C. ^bExact shifts could not be determined due to overlap in the spectra but are within the range 1.30–1.90 ppm. ^cWithin the range 1.60–1.80 ppm. ^dWithin the range 2.80–3.10 ppm. ^eWithin the resonances centered at 7.50, 7.64, or 7.80 ppm. ^fChemical shift could not be determined.

NMR spectrum of the peptide exhibits broad resonances (4.6–13.2 Hz) that, upon denaturation with acetone, narrow to 1.0–2.3 Hz and change in chemical shift to values approximating those expected in a random coil. The two histidines in the peptide (30 and 36) exhibit similar pK_a values (6.5) but show different chemical shifts of the C2 proton resonances, as found in the intact enzyme (Fry et al., 1985). Both tyrosines show hindered rotation and differing environments for the individual ortho and meta aromatic protons (Figure 3). Further, the observation that the peptide is able to bind MgATP and hold it in a relatively high-energy conformation suggests that it possesses a globular, three-dimensional structure.

It is observed in the present study that the resonances of the peptide show a variety of chemical shift values, even among groups of the same residue type, which is further indicative of a defined globular structure. There is also chemical shift heterogeneity among like protons that, in a random structure undergoing rapid conformational averaging, would be equivalent, such as the ring protons of the tyrosine and phenyl-

alanine residues, the CaH protons of glycine residues, and numerous CβH₂ protons.

The secondary structure along the backbone of peptide 1–45 can be discerned by examining the patterns of NOE connectivities between neighboring residues (Figure 8), since these depend in a correlated manner upon the dihedral angles present. Statistical examinations of protein structure (Wüthrich et al., 1984) and model studies (Wüthrich et al., 1984; Wüthrich, 1986) have shown that close NH–NH distances are associated with dihedral angles characteristic of α -helices and that close NH–CaH interresidue distances are associated with dihedral angles characteristic of β -strands. NH–CβH NOEs are also often indicative of α -helix-type dihedral angles. Clearly observed NOEs in the present investigation represent an interproton distance of approximately 3 Å or less on the basis of model studies and on the lack of simultaneous expression of both α -helical and β -like sequential NOEs for most residues. Even at this level of discrimination, the sequential NOEs alone are not diagnostic of secondary structure; however, a segment in which several such NOEs

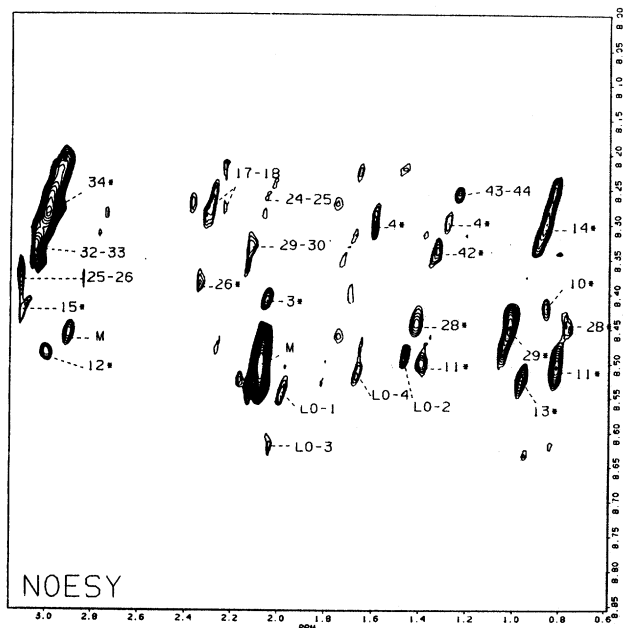


FIGURE 7: Region of NOEs between NH protons and C β H, C γ H, and C δ H protons in the NOESY spectrum of peptide 1-45. Sequential $d_{\beta N}$ NOEs between the C β H of residue i and the NH of residue $i + 1$ are designated $i - (i + 1)$. NOEs identified by a single number and asterisk represent intraresidual effects, which are listed in Table II. NOEs identified by a number preceded by LO represent non-sequential interresidual effects, which are listed by corresponding number in Table II. Cross-peaks labeled M align with resonances of β -mercaptoethanol and may be partially or totally noise artifacts.

of the same type are repeated is suggestive of a region of regular secondary structure (Williamson et al., 1984; van de Ven & Hilbers, 1986; Wüthrich et al., 1984; Holak & Prestegard, 1986). In Figure 8, coherent stretches of a given type of NOE connectivity have been denoted with symbols implying the presence of β -strand or α -helical structure. Regions exhibiting a mixture of connectivities or those that include numerous glycine residues or proline for which the NOE correlations are not clear, are possibly loops, irregular forms of helical structure, or unstructured, flexible regions.

The NMR data suggest that the secondary structure of peptide 1-45 (Figure 8) consists of three stretches of β -strand (residues 8-15, 30-32, and 35-40) and two helical regions (residues 4-7 and 23-29). This is similar but not identical with the distribution of secondary structure found for residues 1-45 in the X-ray structure of adenylate kinase. A residue-by-residue comparison (Figure 8) indicates that 17 of 40 residues or 42% of the residues of the peptide show NOEs in solution consistent with the respective ϕ and ψ angles found in the crystalline enzyme. The remaining five residues of the peptide could not be rigorously compared due to location at the N terminus (Met-1), lack of NH (Pro-17), or diagnostic NOEs that were obscured by other signals (Glu-3, Val-29, Leu-42).

The detailed comparison of the observed NOEs versus those expected if the peptide were rigid and exactly conformed to the X-ray structure thus shows reasonable agreement (Figure 8). One difference, the absence of helix in the peptide for residues 41-45, is apparently due to flexibility at the terminus of the peptide; in the enzyme this helix continues from residue 41 to residue 48. The only substantial differences occurred among residues 17-19 and 29-34 and a marked absence of $d_{\beta N}$ NOEs throughout the peptide. This calculation also validates the expectation of observing either a $d_{\alpha N}$ or a d_{NN} NOE between residues and reveals that the absence of both of these sequential NOEs is often consistent with the X-ray structure.

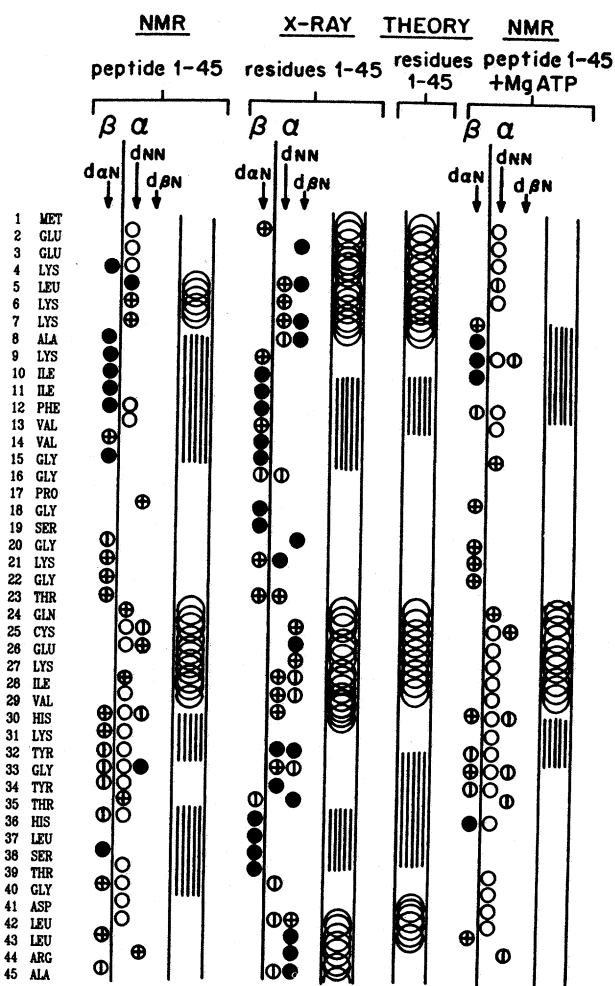


FIGURE 8: Secondary structural determination of peptide 1-45 and the MgATP-peptide 1-45 complex by NMR spectroscopy and comparisons to X-ray and theoretical studies of residues 1-45 in adenylate kinase. Sequential NOEs from NOESY experiments (Figures 5-7) are presented as a series of circles positioned between the two residues that produced the effect. The sequential NOEs designated $d_{\alpha N}$, d_{NN} , and $d_{\beta N}$ represent effects between the NH proton of residue i and, respectively, the C α H, NH, or C β H proton of residue $i - 1$. These NOEs are segregated on the basis of being typically indicative of β -strand structure ($d_{\alpha N}$) or α -helical structure (d_{NN} , $d_{\beta N}$) (Wüthrich et al., 1984; Wüthrich, 1986). An annotated circle represents an observed NOE, with a relative magnitude that is small (ϕ), medium (\otimes), or large (\bullet). Open circles represent NOEs that would not be observable due to overlap with the diagonal in the NOESY spectrum. Regions of proposed coherent secondary structure from analysis of NOE connectivities are designated by overlapping circles for α -helix and vertical lines for β -strand. The X-ray data are taken from the structure of residues 1-45 in porcine muscle adenylate kinase (Sachsenheimer & Schulz, 1977). The porcine sequence differs from that of peptide 1-45 as follows: residue 8 = Ser and residue 30 = Gln. The pattern of NOEs depicted under the X-ray heading are the effects that would be expected if the peptide maintained a rigid structure identical with that of residues 1-45 in the enzyme. These NOEs were calculated by adding protons to the X-ray structure following standard geometries using the computer program AFFIX, written by Wayne Hendrickson. Small, medium, and large NOEs were assigned to pairs of protons calculated to be 2.71-3.00, 2.41-2.70, and 1.70-2.40 Å apart, respectively. The theoretical structure assessment is that obtained by applying the predictive algorithm of Chou and Fasman (1974) to the sequence.

The peptide seems to have adopted a structure that its amino acid sequence has a strong tendency toward forming on the basis of Chou-Fasman calculations (Chou & Fasman, 1974) (Figure 8, Table III).

Structural Information from NMR Spectroscopy: Tertiary Structure. There were numerous NOEs of the nonsequential

SOLUTION STRUCTURE OF MGATP-BINDING PEPTIDE

 Table II: Nonsequential NOEs Involving the NH Region in the Free Peptide and the Peptide-MgATP Complex Together with Tentative Assignments^a

intraresidual NOEs	obsn in peptide-MgATP complex ^b	interresidual NOEs ^c	obsn in peptide-MgATP complex ^b
Peptide			
E3 NH-E3 C β H	E	LO-1 L5 NH-M1 C β H ₂ ^d	X
K4 NH-K4 C β H	X	LO-2 F12 NH-I10 C γ H ₂ ^d	X
K4 NH-K4 C γ H ₂	X	LO-3 G22 NH-Q24 C β H ₂ ^d	E
K7 NH-K7 C α H	E	LO-4 H30, C2H-K31 C δ H ₂	X
I10 NH-I10 C γ H ₃	X		
I11 NH-I11 C γ H ₂	L		
I11 NH-I11 C γ H ₃	S		
F12 NH-F12 C β H	X		
V13 NH-V13 C γ H ₃	E		
V14 NH-V14 C γ H ₃	S		
G15 NH-G15 C α H	E		
G22 NH-G22 C α H	E		
E26 NH-E26 C γ H ₂	L		
I28 NH-I28 C γ H ₂	E		
I28 NH-I28 C γ H ₃	X		
V29 NH-V29 C β H	X		
V29 NH-V29 C γ H ₃	S		
Y34 NH-Y34 C β H	S		
L42 NH-L42 C β H	X		
R44 NH-R44 C α H	X		
Additional NOEs in the Peptide-MgATP Complex			
K6 NH-K6 C β H		G18 NH-P17 C γ H ₂	
I10 NH-I10 C γ H ₂		R44 NH-L43 C δ H ₃	
I11 NH-I11 C β H		MgATP H2-L37 C β H	
G15 NH-G15 C α H		MgATP H8-MgATP H2'	
G16 NH-G16 C α H		MgATP H8-MgATP H3'	
K21 NH-K21 C γ H ₂		MgATP H8-V13, Q24, or V29 C β H	
T23 NH-T23 C γ H ₃		MgATP H8-I28 C δ H ₃	
L43 NH-L43 C δ H ₃			

^aFrom Figures 5 and 7. ^bX indicates that the NOE was not observed in the peptide-MgATP complex; other letters indicate that the NOE was observed in the complex and was larger (L), smaller (S), or equal (E) in magnitude to the comparable effect in the peptide alone. ^cNumbers preceded by LO- correspond to the labeling used for long-range NOEs in Figure 7. ^dThis interresidual proton pair is ≤ 4.0 Å apart in the X-ray structure of residues 1-45 in adenylate kinase to which protons have been affixed.

type observable in the NOESY spectra of the peptide, which are listed in Table II and can be seen in Figures 5 and 7. Due to crowding, NOEs in the aliphatic region of the spectrum were not considered. Most of the nonsequential NOEs could be explained as intraresidual effects. Potential assignments for NOEs that could not be assigned as intraresidual effects were evaluated by calculating all possible nonsequential NOEs (pairs of protons < 4 Å apart) using the X-ray structure of residues 1-45 with protons affixed to it (see Figure 8 legend). Three nonsequential effects were consistent with proximities observed in the X-ray structure. The remaining observed long-range effect could not be evaluated by this method, since it involved the His-30 C2H resonance and the X-ray structure is of the porcine enzyme that has a glutamine at position 30. The available set of long-range NOEs (Table II) does not provide enough information for a unique determination of the tertiary structure. However, these NOEs, together with previously determined distances from Cr³⁺ATP to peptide protons, and intermolecular NOEs from the peptide to

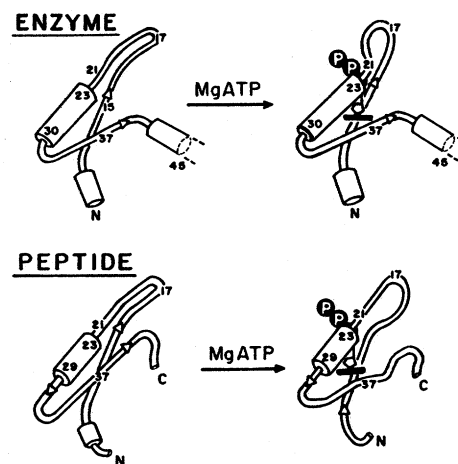


FIGURE 9: Comparison of structures of residues 1-45 in the X-ray structure of adenylate kinase in the absence and presence of MgATP (Pai et al., 1977; Sachsenheimer & Schulz, 1977) with structures of the peptide suggested by the NOE data. The location of MgATP is based on NMR studies (Fry et al., 1985). Changes in the peptide conformation induced by MgATP binding are suggested by changes in the sequential (Figure 8) and interresidual NOEs (Table II).

MgATP (Fry et al., 1985) are consistent with the tertiary structure found by X-ray for residues 1-45 of the entire enzyme (Figure 9), including the conformation of the glycine-rich loop recently described at 2.1-Å resolution (Dreusicke & Schulz, 1986). The lack of long-range C α H_i-NH_{i+3} NOEs and C α H_i-C β H_{i+3} NOEs and the small number of C β H_i-NH_{i+1} NOEs typically found for α -helices (Table II) are most likely due to irregularity or flexibility of the peptide structure. It has been shown for peptides which are rigidly α -helical in a stabilizing methanol/water solvent that reduction in methanol concentration is accompanied by the loss of long-range C α H_i-C β H_{i+3} NOEs, while the NH_i-NH_{i+1} backbone NOEs, indicative of α -helical conformation, are maintained (Fry et al., 1988). In addition, the absence of remote C α H-C α H cross-strand NOEs in peptide 1-45, typically observed for extended β -sheet structure (van de Ven & Hilbers, 1986a; Williamson et al., 1984) indicates that the proposed β -strands are not tightly associated in an extended β -sheet.

Structural Information from FTIR Spectroscopy. For typical globular proteins, resolution enhancement of the IR spectrum reveals that the amide I band consists of six to nine overlapping components, some of which are detected only by curve fitting (Byler & Susi, 1986; Surewicz et al., 1987; Surewicz & Mantsch, 1988). By contrast, for casein proteins (Susi & Byler, 1988) and for the 45-residue peptide and its ATP complex, resolution enhancement neither by second derivatives (Susi & Byler, 1983) nor by deconvolution (Yang et al., 1985; Byler & Susi, 1986) yielded spectra in which individual amide I band components could be observed. This indicates that the secondary structure of the peptide is somewhat disordered, compared to that of the enzyme, which is consistent with the positive sign of the NOEs (Fry et al., 1985). However, the unusual width and asymmetry of the observed amide I band of the peptide (Figure 10), similar to those found for many globular proteins (Byler & Susi, 1986; Susi & Byler, 1988), indicates that this band is a composite of multiple components. Assuming this to be the case, we fit the spectra of Figure 10 as previously described, using the average frequencies of the five principal components that characterized the secondary structures of 17 globular proteins (Byler & Susi, 1986). The frequencies were fixed to 1654 cm⁻¹ for α -helices, 1633 and 1675 cm⁻¹ for β -chains, 1663 cm⁻¹ for turns, and 1645 cm⁻¹ for unordered or aperiodic segments, and

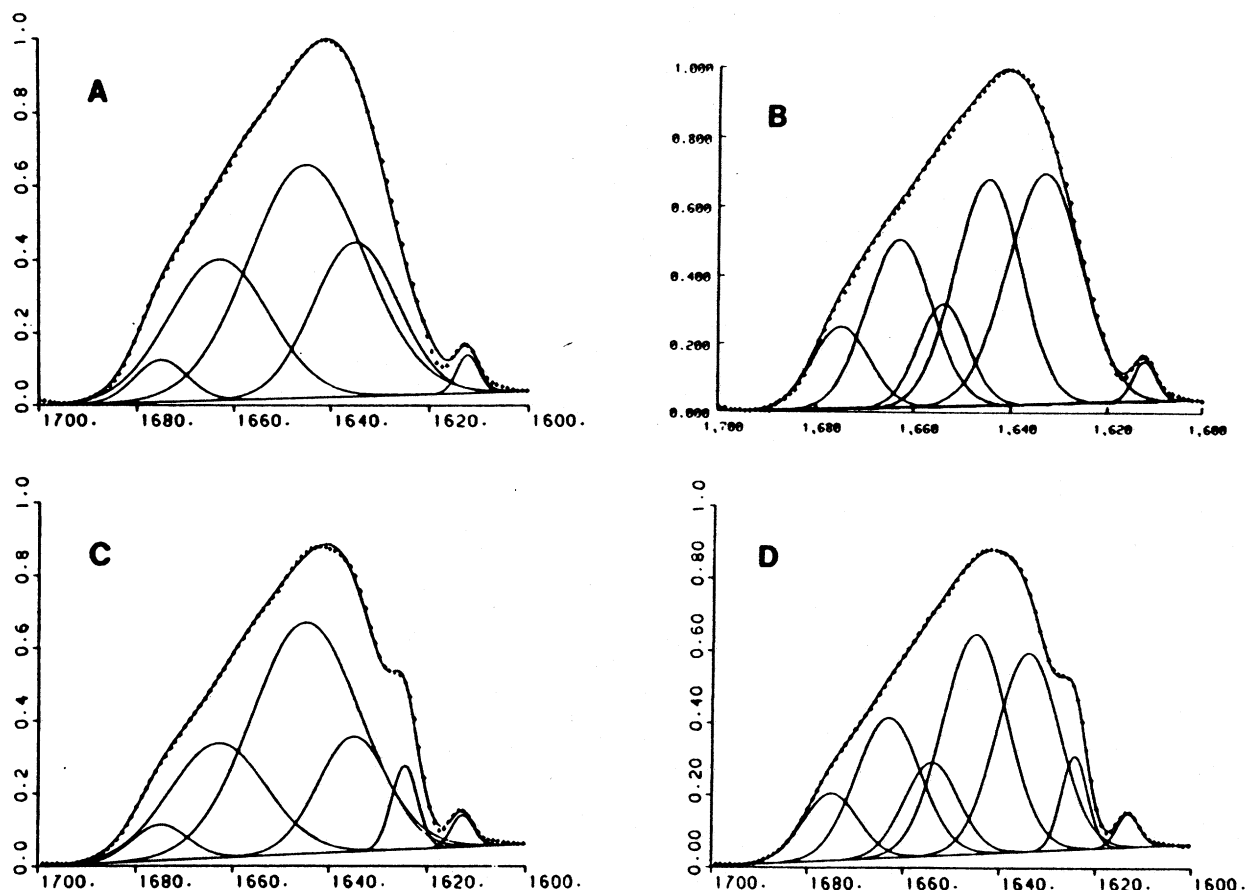


FIGURE 10: FTIR spectra of the 45-residue peptide (A and B) and its 1:1 mole ratio complex with MgATP (C and D) in the amide I region. Relative absorbance is plotted versus wavenumber frequency (cm^{-1}). Crosses (+) represent the deconvolved experimental data; the solid lines (—) give both the individual calculated components and the calculated sum of the components. (Because the deviation between the calculated curve and the experimental data is so small, the former is virtually superimposed upon the latter.) In (A) and (C), the height of the amide I band corresponding to α -helices (1654 cm^{-1}) was constrained to zero. In the other two spectra [(B) and (D)], the heights and widths of all component bands were allowed to iterate to the best fit.

Table III: Comparison of Secondary Structures of Peptide 1–45 Determined by NMR, FTIR, and CD Spectroscopy, X-ray of Complete Protein, and Theoretical Calculations

structural contribution	peptide alone					peptide + MgATP		
	NMR	X-ray	theor ^a	FTIR ^b	CD	NMR	FTIR ^b	CD
α (%)	24	47	42	$\leq 10^c$	5–13	20	$\leq 15^c$	2–10
β (%)	38	22	24	27–42 ^c	22–26	22	27–38 ^c	21–25
other ^d (%)	38	31	34	48 ^c –73	62–70	58	47 ^c –73	66–74

^a Estimated as described by Chou and Fasman (1974). ^b The range of values results from the use of both the four-parameter and five-parameter fits (c) as described in the text. Because the characteristic frequencies used to calculate the FTIR percentages are average values, accurate only to about $\pm 2\text{--}3 \text{ cm}^{-1}$, the calculated contributions themselves have an error of approximately $\pm 10\%$ of the values shown. ^d Includes turns and aperiodic structure.

all bandwidths and intensities were allowed to vary.

In all of the spectra (Figure 10), the weak band observed at approximately 1612 cm^{-1} is not an amide I component but is due to the ring-stretching vibration of aromatic side chains, as is found in most proteins (Byler & Susi, 1986). While the FTIR method has previously been applied only to globular proteins (Byler & Susi, 1986; Susi & Byler, 1987; Surewicz et al., 1987; Surewicz & Mantsch, 1988), the validity of its use in the present case with peptides is supported by the results of the curve-fitting procedure, which yielded bandwidths and intensities of the individual components comparable to those found for proteins. The data could be fit by omitting the α -helical component (Figure 10A). However, a much better fit, with a significantly lower error, was obtained by including the α -helical band (Figure 10B). The sizable variation in the conformation calculated by FTIR (Table III) reflects the results of these alternative fits, but the overall structure, independently determined by FTIR, is similar to that found by

NMR and CD (Table III). The β -strand content agrees with that suggested by NMR, but the amount of α -helix indicated by the FTIR analysis is less than that estimated by NMR. Empirically, the FTIR technique is somewhat insensitive to helices, especially very short ones (< 6 residues) in which too few carbonyl groups are coupled to yield a strong absorption. Such an explanation seems especially plausible, since peptides that are truly nonstructured are typified by, in addition to featureless CD spectra, an almost total lack of sequential NOEs (Clore et al., 1986).

Structural Information from CD Spectroscopy. The CD spectrum of the peptide at 25°C (Figure 10) is relatively featureless and, in particular, shows little helical content. Following the method of Stone et al. (1985), basis sets for four structures at a time were compared to the spectrum. Each set included the following: one type of helix, long or short helix derived from protein spectra or a short helix derived from peptide spectra; one type of β -structure derived from protein

Table IV: Altered Chemical Shifts of Peptide Resonances and Chemical Shift Values for MgATP Resonances in the Peptide-MgATP Complex

peptide resonance	chemical shift in MgATP-peptide complex ^a	Δ ppm from value in free peptide	MgATP resonance	chemical shift
Lys-4 NH	8.27	-0.02	ribose H1'	6.12
Lys-6 CaH	4.27	-0.02	ribose H2'	4.77
Lys-9 NH	8.28	-0.02	ribose H3'	4.58
Val-13 C γ H ₃	0.99	+0.04	ribose H4'	4.41
Ser-19 CaH	4.44	-0.02	ribose H5',5''	4.26
NH	8.34	+0.05	adenine H2	8.22
Lys-21 CaH	4.34	-0.02	adenine H8	8.51
Gln-24 CaH	4.48	+0.02		
NH	8.24	+0.02		
Cys-25 NH	8.27	+0.02		
Lys-27 CaH	4.28	-0.02		
NH	8.46	+0.23		
Lys-31 CaH	4.14	+0.02		
Tyr-32 NH	8.27	+0.02		
Gly-33 NH	8.33	-0.03		
Leu-42 NH	8.35	+0.02		
Arg-44 CaH	4.34	-0.03		
NH	8.33	+0.07		

^aChemical shifts are reported in ppm from external DSS. The sample was at pH 5.6 and 10 °C.

or peptide spectra; a β -turn component; and either an extended or a collapsed nonordered structure (Stone et al., 1985; Chang et al., 1978). The best fits were obtained with the set that included short helices and β -structures derived from peptides and extended nonordered structures. Estimates of secondary structure obtained from the spectrum of the peptide alone were at most 13% helix, 22–26% β , and 62–70% aperiodic structure (Table III). Lowering the temperature to 10 °C did not significantly alter the CD spectrum (not shown) or the parameters used to fit it.

Apparently the two regions of successive α -helical sequential NOEs detected by NMR, a low-frequency technique that yields an average structure, are too short or too kinked or possess too much internal motion and disorder to yield parameters at high frequencies, in CD and FTIR spectra, characteristic of α -helices found in larger proteins, including adenylate kinase (Monott et al., 1987). Floppiness of this peptide is indicated by the positive NOEs from peptide protons to those of bound MgATP and within bound MgATP (Fry et al., 1985) and by the small number of long-range NOEs (Table II).

Structural Information on the Peptide-MgATP Complex. The binding of MgATP caused significant structural changes in the peptide as detected by NMR. The chemical shifts of numerous protons were altered, as listed in Table IV. There were fewer sequential NOEs observed, and their distribution was different, as shown in Figure 8. The NOE pattern for the peptide with MgATP bound indicates disruption of the helical structure at residues 4–7 and the β -strand at residues 35–40 and shortening of the β -strand at residues 8–15 to residues 7–12. The set of observed nonsequential NOEs was also altered, as shown in Table II. Among the new NOEs that appear upon binding of MgATP are several which apparently are intermolecular effects. Again, the nonsequential NOEs are insufficient to provide a unique description of the tertiary structure of the peptide that has bound MgATP. Nevertheless, the data are consistent with the structural changes shown in Figure 9, which are comparable to those induced by the binding of MnATP to the complete enzyme as determined by X-ray analysis (Pai et al., 1977).

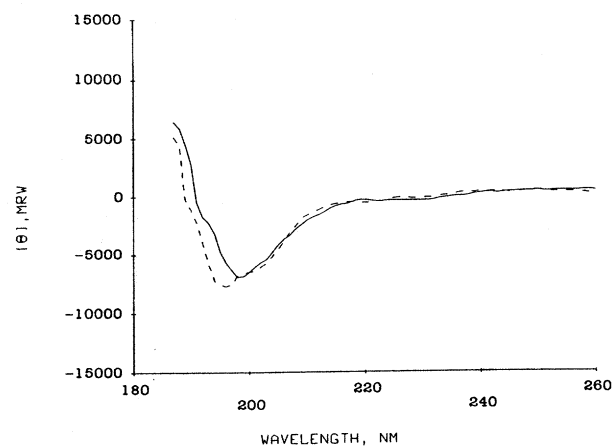


FIGURE 11: Far-ultraviolet circular dichroism spectra of rabbit muscle adenylate kinase synthetic peptide 1–45 (—) and its complex with MgATP (---). The peptide solution 320 μ M in 0.03 M NaCl, pH 5.6, was placed in a cylindrical cell of 0.02-cm path length. $[\theta]_{MRW}$ is the mean residue ellipticity in degrees.

For the ATP complex of the 45-residue peptide (Figure 10C,D), resolution-enhanced FTIR spectra revealed the purine ring stretching mode of the ATP at 1624 cm^{-1} but detected no significant changes in the peptide structure (Figure 10C,D, Table III).

In the CD spectrum of the peptide, the addition of MgATP caused a slight increase in negative ellipticity and a shift toward lower wavelength of 2–3 nm for the CD minimum at 25 °C (Figure 11). The CD spectrum of the MgATP complex of the peptide was not altered further by lowering the temperature to 10 or 2 °C. The binding of MgATP did not cause a significant change in the structural parameters used to fit the CD spectrum (Table III), although there was a slight decrease in helicity in accord with the NMR data. It is likely that structural features detected by NMR, which were eliminated upon binding of MgATP, may have already been too irregular to be recognized in the analysis of the CD spectrum.

The present study provides new information on the location of bound MgATP and its effects on the structure of the peptide and allows an evaluation of conclusions and assumptions made in the previous work (Fry et al., 1985). MgATP was previously considered to be bound in a region of the peptide encompassing residues 13–37, and observed 1-D intermolecular NOEs were assigned as (1) ATP H8–Ile-28 C γ H₃, (2) H8–Ile-28 C β H, (3) H2–Leu-37 C δ H₃, and (4) H2–Leu-37 C γ H. The present detailed assignments of the peptide resonances suggest that effect 1 involves Ile-28 C γ H₂, and that effects 3 and 4 involve the two Leu-37 C β H resonances. Effect 2 apparently does not involve a resonance of Ile-28 but instead is assignable as the C β H of Glu-3, Val-13, or Val-29. NOE 4 was observed in the 2-D NOESY spectrum; NOE 2 would be obscured by noise from the β -mercaptoethanol resonance. An additional intermolecular NOE was observed in the present study, assignable as ATP H8–Ile-28 C δ H₃. These findings are consistent with the previously determined MgATP binding site (Fry et al., 1985). The reassigned intermolecular NOE is accounted for by the proximity of adenine H8 to Val-13, Gln-24, and Val-29. In the proposed binding site, MgATP is located between the α -helix composed of residues 23–30 and the β -strand 35–39. The helix appears to be maintained in the peptide when it is complexed with MgATP; the β -strand is disrupted (Figures 8 and 9). Most of the chemical shift changes observed upon binding of MgATP involve residues proposed to be at or near the binding site (13, 21, 24, 25, 27, 31, 32, 33) (Table IV). Overall, the present NMR data agree

with the previously proposed binding site of MgATP on the peptide and on the enzyme.

ACKNOWLEDGMENTS

We thank Peter Demou at the New England NMR Facility at Yale University for his help in obtaining and processing NMR data on the Bruker WM-500 spectrometer and Dr. Dennis Hare for allowing use of his FTNMR program. We also thank Dr. Eric Suchanek for analysis of the adenylate kinase X-ray structure, Dr. Wayne Hendrickson at Columbia University for allowing use of his AFFIX program, Dr. Alan Frankel for assistance in applying the Chou-Fasman algorithms, and Dr. David Shortle for permitting use of his spectropolarimeter.

Registry No. MgATP, 1476-84-2; rabbit muscle adenylate kinase (1-45), 113685-56-6; adenylate kinase, 9013-02-9.

REFERENCES

- Anil Kumar, Ernst, R. R., & Wüthrich, K. (1980) *Biochem. Biophys. Res. Commun.* **95**, 1-6.
- Aue, W. P., Bartholdi, E., & Ernst, R. R. (1976) *J. Chem. Phys.* **64**, 2229-2246.
- Bax, A., & Freeman, R. (1981) *J. Magn. Reson.* **44**, 542-561.
- Bolotina, I. A., Chekhov, V. O., Lugauskas, V. Yu., Finkel'shtein, A. V., & Ptitsin, O. B. (1980) *Mol. Biol.* **14**, 701-709.
- Bundi, A., & Wüthrich, K. (1979) *Biopolymers* **18**, 285-297.
- Byler, D. M., & Susi, H. (1986) *Biopolymers* **25**, 469-487.
- Chang, C. T., Wu, C.-S. C., & Yang, J. T. (1978) *Anal. Biochem.* **91**, 13-31.
- Chen, G. C., & Yang, J. T. (1977) *Anal. Lett.* **10**, 1195-1207.
- Chen, Y.-H., Yang, J. T., & Chau, K. H. (1974) *Biochemistry* **13**, 3350-3359.
- Chou, P. Y., & Fasman, G. D. (1974) *Biochemistry* **13**, 222-244.
- Clore, G. M., Martin, S. R., & Gronenborn, A. M. (1986) *J. Mol. Biol.* **191**, 553-561.
- Dreusicke, D., & Schulz, G. E. (1986) *FEBS Lett.* **208**, 301-304.
- Fry, D. C., Kuby, S. A., & Mildvan, A. S. (1985) *Biochemistry* **24**, 4680-4694.
- Fry, D. C., Kuby, S. A., & Mildvan, A. S. (1986a) *Proc. Natl. Acad. Sci. U.S.A.* **83**, 907-911.
- Fry, D. C., Byler, D. M., Susi, H., Brown, E. M., Kuby, S. A., & Mildvan, A. S. (1986b) *Fed. Proc., Fed. Am. Soc. Exp. Biol.* **45**, 1517.
- Fry, D., Greeley, D., Berkovitch-Yellin, Z., Madison, V., Toome, V., Felix, A., & Heimer, E. (1988) *FASEB J.* **2**, A1336.
- Hamada, M., Palmieri, R. H., Russell, G. A., & Kuby, S. A. (1979) *Arch. Biochem. Biophys.* **195**, 155-177.
- Holak, T. A., & Prestegard, J. H. (1986) *Biochemistry* **25**, 5766-5774.
- Jeener, J., Meier, B. H., Bachmann, P., & Ernst, R. R. (1979) *J. Chem. Phys.* **71**, 4546-4553.
- Macura, S., Huang, Y., Suter, D., & Ernst, R. R. (1981) *J. Magn. Reson.* **43**, 259-281.
- Marion, D., & Wüthrich, K. (1983) *Biochem. Biophys. Res. Commun.* **113**, 967-974.
- Monott, M., Gilles, A.-M., Gerons, I. S., Michelson, S., Barzu, O., & Femandjian, S. (1987) *J. Biol. Chem.* **262**, 2502-2506.
- Pai, E. F., Sachsenheimer, W., Schirmer, R. H., & Schulz, G. E. (1977) *J. Mol. Biol.* **114**, 37-45.
- Sachsenheimer, W., & Schulz, G. E. (1977) *J. Mol. Biol.* **114**, 23-26.
- Stone, A. L., Park, J. Y., & Martenson, R. E. (1985) *Biochemistry* **24**, 6666-6673.
- Surewicz, W. K., & Mantsch, H. H. (1988) *Biochim. Biophys. Acta* (in press).
- Surewicz, W. K., Moscarello, M. A., & Mantsch, H. H. (1987) *Biochemistry* **26**, 3881-3886.
- Susi, H., & Byler, D. M. (1983) *Biochem. Biophys. Res. Commun.* **115**, 392-397.
- Susi, H., & Byler, D. M. (1987) *Arch. Biochem. Biophys.* **258**, 465-469.
- Susi, H., & Byler, D. M. (1988) *Appl. Spectrosc.* (in press).
- van de Ven, F. J. M., & Hilbers, C. W. (1986a) *J. Mol. Biol.* **192**, 419-441.
- van de Ven, F. J. M., & Hilbers, C. S. (1986b) *J. Mol. Biol.* **192**, 389-417.
- Wagner, G., & Wüthrich, K. (1982) *J. Mol. Biol.* **155**, 347-366.
- Wagner, G., Neuhaus, D., Wörgötter, E., Vašák, M., Kagi, J. H. R., & Wüthrich, K. (1986) *Eur. J. Biochem.* **157**, 275-289.
- Wand, A. J., & Englander, S. W. (1986) *Biochemistry* **25**, 1100-1106.
- Weber, P. L., Wemmer, D. E., & Reid, B. R. (1985a) *Biochemistry* **24**, 4553-4562.
- Weber, P. L., Drobny, G., & Reid, B. R. (1985b) *Biochemistry* **24**, 4549-4552.
- Williamson, M. P., Marion, D., & Wüthrich, K. (1984) *J. Mol. Biol.* **173**, 341-359.
- Williamson, M. P., Havel, T. F., & Wüthrich, K. (1985) *J. Mol. Biol.* **182**, 295-315.
- Wüthrich, K. (1986) *NMR of Proteins and Nucleic Acids*, Wiley, New York.
- Wüthrich, K., Billeter, M., & Braun, W. (1984) *J. Mol. Biol.* **180**, 715-740.
- Yang, W.-J., Griffiths, P. R., Byler, D. M., & Susi, H. (1985) *Appl. Spectrosc.* **39**, 282-287.